Solar-Terrestrial Physics. 2025, vol. 11, iss. 2, pp. 88–98. DOI: 10.12737/stp-112202509. © 2025 A.Yu. Gololobov, I.A. Golikov, V.I. Popov. Published by INFRA-M Academic Publishing House

DOI: 10.12737/stp-112202509

Received September 16, 2024
Accepted January 14, 2025

MODELLING THE INFLUENCE OF MAGNETOSPHERIC STORM ON THE LARGE-SCALE STRUCTURE OF THE HIGH-LATITUDE IONOSPHERE FOR WINTER SOLSTICE CONDITIONS

A.Yu. Gololobov
Yu.G. Shafer Institute of Cosmophysical Research and Aeronomy SB RAS, Yakutsk, Russia, Gololobov@ikfia.ysn.ru

I.A. Golikov
Yu.G. Shafer Institute of Cosmophysical Research and Aeronomy SB RAS, Yakutsk, Russia, gia2008n@mail.ru

V.I. Popov
Yu.G. Shafer Institute of Cosmophysical Research and Aeronomy SB RAS, Yakutsk, Russia, volts@mail.ru

Abstract. Using numerical calculations with a model of the high-latitude ionosphere in Eulerian variables, we study the influence of magnetospheric convection on the large-scale structure of the ionosphere during a moderate geomagnetic storm for winter solstice conditions. The perturbed electric field of convection is shown to cause changes in the shapes and sizes of the main structural formations of the ionosphere. We have found out that the effect of a geomagnetic storm depends on the time of the beginning of the disturbance due to the displacement between the geographic and geomagnetic poles (UT control). The effect is most pronounced in the case of a storm that begins at 16 UT, when the perturbed electric field of magnetospheric convection transfers plasma of the daytime ionosphere to the nightside. It is shown that during periods of disturbances along with the horizontal component of the electromagnetic drift its vertical component, which causes an increase in the height of the F2-layer maximum on the dayside and its decrease on the nightside, also has a significant effect.

Keywords: magnetospheric convection, magnetic storm, ionosphere model, high-latitude ionosphere, subauroral ionosphere, mismatch of poles.

INTRODUCTION

The high-latitude ionosphere exhibits regular large-scale structural features such as the tongue of ionization and the polar hole at high latitudes, polar and auroral peaks in the dayside cusp and in the night sector, as well as the main ionospheric trough (MIT) at subauroral latitudes [Mizun, 1980]. During geomagnetic storms, configuration of these features gets much more complicated, which is mainly caused by perturbation of the large-scale electric field of magnetospheric convection that depend on the orientation of the interplanetary magnetic field (IMF). Depending on IMF orientation, magnetospheric convection can have a two-vortex, three-vortex, and four-vortex structure [Heppner, Maynard, 1987]. IMF variations during storms define the unsteady nature of convection and cause the large-scale structure of the ionosphere to change significantly. The ionospheric response to geomagnetic storms is most pronounced during the storm main phase. There are positive and negative ionospheric disturbances that lead to a local increase and decrease in electron density n_e respectively [Prölss, 1995; Danilov, 2013; Ratovsky et al., 2018; Klimenko et al., 2015]. Changes in n_e distribution during geomagnetic storms affect radio wave propagation and positioning accuracy of global navigation satellite systems.

The effect of the convection electric field on the large-scale structure of the high-latitude ionosphere during disturbed periods has been repeatedly studied using numerical models [Klimenko, Namgaladze, 1976; Mingalev, 1978; Zherebtsov et al., 1988; Uvarov, Barashkov, 1989; Tashchilin, Romanova, 2002, 2007; Uvarov, Lukianova, 2014; Uvarov, Lukianova, 2015; Lukianova et al., 2016; Liu et al., 2017; Larina, Glebova, 2019; Klimenko et al., 2019]. The first works on the effect of magnetospheric convection employed models based on the Lagrange formalism under the assumption that the geographic and geomagnetic poles coincide. In [Uvarov, Lukianova, 2014; Uvarov, Lukianova, 2015], the convection effect of various types on the structure of the high-latitude ionosphere was examined and it was shown that a change in the IMF orientation leads to a restructuring of the large-scale structure of the high-latitude ionosphere. Later, a study was conducted on the IMF effect on the large-scale structure of the high-latitude ionosphere, taking into account the displacement between geographic and geomagnetic poles under stationary conditions [Lukianova et al., 2016]. Larina, Glebova [2019] analyzed the response of the high-latitude ionosphere to an abrupt change of the sign of the IMF B_y component and found that the change of the sign of B_y is followed by stratification of the tongue of ionization and by formation of large-scale blobs of ionization. Deng and Ridley [2006] investigated the ionospheric response to a sudden disturbance of the convection electric field at 12:00 UT, using the numerical model GITM (Global Ionosphere-Thermosphere Model) and the Weimer electric field model [Weimer, 1996]. They found that the vertical component of the **E×B**-drift velocity vector causes the F2

layer to move upward in the dayside ionosphere and to move downward on the nightside, which was also observed in [Klimenko, Namgaladze, 1976; Mingalev, 1978]. Liu et al. [2017] used the Thermosphere–Ionosphere Electrodynamic General Circulation Model (TIEGCM) to examine the configuration of the tongue of ionization at different IMF parameters at different moments of UT. Klimenko et al. [2019] employed the Global Self-consistent Model of the Thermosphere, Ionosphere, and Protonosphere (GSM TIP) to analyze the structure of the tongue of ionization during the March 16–18, 2015 geomagnetic storm (St. Patrick's Storm). Note that the above studies [Deng, Ridley, 2006; Liu et al., 2017; Klimenko et al., 2019, etc.] were carried out for equinox conditions. Meanwhile, the effects of displacement between the poles are most pronounced for winter conditions [Kolesnik, Golikov,1982, 1984; Golikov et al., 2020; Golikov et al., 2022]. In this regard, it is interesting to examine the effect of magnetospheric convection on the large-scale structure of the high-latitude ionosphere during a geomagnetic storm for winter solstice conditions (δ=–23°).

The purpose of this work is to study the effect of the perturbed magnetospheric convection electric field on the large-scale structure of the ionosphere during a geomagnetic storm in winter, using a nonstationary ionospheric model constructed taking into account the displacement between geographic and geomagnetic poles. To account for the convection, we employ the Weimer empirical model of the electric potential of the high-latitude ionosphere [Weimer, 1996]. The Weimer model is based on spherical harmonic functions whose coefficients were derived from satellite data, and allows us to obtain the electric field potential distribution in the high-latitude ionosphere depending on IMF parameters.

1. MODEL OF THE HIGH-LATITUDE IONOSPHERE

The calculations have been carried out by the model of the high-latitude F-region of the ionosphere, whose equations are written in Eulerian variables in a spherical geographic coordinate system with a polar axis coinciding with Earth's rotation axis [Golikov et al., 2012, 2016]. The electron density n_e, temperatures of electrons T_e and ions T_i in the height range 120–1000 km are determined by numerically solving a system of nonstationary three-dimensional equations consisting of equations of continuity for ions and thermal conductivity for electrons and ions. In the height range considered, the quasi-neutrality condition can be assumed, i.e. $n_e \approx \sum n_i$. Cooling rates of electron gas when interacting with neutral particles and ions are set according to [Schunk, Nagy, 1978; David et al., 2011]. The temperature and concentration of neutral components were calculated using the thermosphere model NRLMSISE-00 [Picone et al., 2002]. We employed the Auroral Precipitation Model (APM) [Vorobjev et al., 2013] to calculate the distribution of average energies and energy fluxes of precipitating electrons, and the formula proposed in [Fang et al., 2008] to find the ion formation function of precipitating particles. The photoionization rates at large zenith angles of the Sun (χ>75°) are computed according to [Chapman, 1931]. The displacement between geographic and geomagnetic poles is taken into account as follows. The electric field and magnetospheric convection velocity components, zones of energetic particle precipitation and downward heat flow are determined in a spherical geomagnetic coordinate system with subsequent transition into a geographic system. We set the coordinates of the north geomagnetic pole 78.5° N, 291° E [Schunk, Nagy, 2009]. The geomagnetic field is defined in the dipole approximation whose components in the spherical coordinate system have the form

$$H_r = -2g_0\left(\frac{R_E}{r}\right)^3 \cos\theta_м,$$

$$H_{\theta_м} = -g_0\left(\frac{R_E}{r}\right)^3 \sin\theta_м,$$

$$H_\varphi = 0,$$

where r is the radius; θ_m is the geomagnetic colatitude; R_E is the Earth radius; g_0~0.3 G is the intensity of the geomagnetic field measured at the equator at $r=R_E$.

The algorithm for solving the system of modeling equations is analyzed in [Golikov et al., 2012, 2016]. To numerically solve the system of three-dimensional differential equations, we employed the total approximation method [Samarskii, 2001] in which the solution of three-dimensional differential equations is reduced to the successive solution of a system of one-dimensional equations. Next, for one-dimensional equations we use a finite difference approximation followed by reduction to a three-point scheme that is solved by the tridiagonal matrix algorithm. A simple Chapman layer is utilized as the initial condition for solving the continuity equation for atomic oxygen ions, and electron and ion temperatures are equated to the neutral gas temperature. The calculations were made as follows: Δr=10 km, $\Delta\theta$=2°, $\Delta\varphi$=10°, Δt=5 min.

A significant problem in modeling the high-latitude ionosphere is to set upper boundary conditions in the region where particles are exchanged with the protonosphere and the inner magnetosphere, especially in the case of disturbances. In this work, a plasmaspheric ion flux O^+ $F=\pm10^8$ cm^{-2} s^{-1} (plus corresponds to the dayside period; minus, to the nightside period) is specified according to [Evans, 1974] behind the convection region, where it is assumed that the field lines are closed. At high latitudes, a zero flux F=0 is assumed in the convection region in accordance with the results of [Kolesnik, Golikov, 1981], where it is shown that in this latitude region n_e at the height of the F2 maximum weakly depends on the flux at the upper boundary.

2. INPUT PARAMETERS

Yermolaev et al. [2011] used OMNI data [http://omniweb.gsfc.nasa.gov] for the period from 1976 to 2000 for statistically studying solar wind and interplanetary magnetic field (IMF) parameters during magnetic storms. The sudden commencement of a moderate geomagnetic storm (from –50 to –100 nT) was shown to occur with a sharp decrease in IMF B_z to about –7 nT within 1–2 hrs during the storm initial phase. Then, during

the main phase there is a slow monotonous decrease in IMF B_z to –8 nT. At the same time, the geomagnetic activity index *Dst* reaches about –80 nT. The storm main phase lasts for ~6 hrs. Variations in IMF B_x and B_y, the solar wind velocity V, and its density N during the moderate storm can be assumed to be insignificant. Using these results, we set the following input parameters of the Weimer model to describe the perturbed electric field during the moderate geomagnetic storm: V≈400 km/s, N≈10 cm^{-3}, B_x≈0 nT, B_y≈0 nT. The IMF B_z component is given by a variable (Figure 1, *a*). There are two diametrically opposite scenarios: 1 — with the onset of the storm at 16 UT; 2 — with the onset of the storm at 04 UT (see Figure 1) since the displacement between geomagnetic and geographic poles leads to UT control of the large-scale structure of the high-latitude ionosphere [Watkins, 1978; Sojka et al., 1979; Kolesnik, Golikov, 1982; Golikov et al., 2016]. The charged particle precipitation model APM PGIA utilizes the geomagnetic activity indices *Dst* and *AL* as input parameters, calculated from the given IMF parameters, using the following expressions [Burton et al., 1975; Murayama et al., 1980; Murayama, 1982]:

$$Dst = Dst_0 + b\left(P\right)^{1/2} - c,$$

$$AL = -60\left(B_s + 0.5\right)\left(V/400\right)^2,$$

where

$$\frac{dDst_0}{dt} = F\left(E\right) - aDst_0;$$

$$F\left(E\right) = \begin{cases} 0, E_y < 0.5 \text{ mV/m}; \\ d\left(E_y - 0.5\right), E_y \geq 0.5 \text{ mV/м}; \end{cases}$$

$$B_s = \begin{cases} 0, B_z \geq 0; \\ -B_z, B_z < 0. \end{cases}$$

Here $E_y = VB_z \cdot 10^{-3}$ [mV m^{-1}], $P = nV^2 \cdot 10^{-2}$ [eV cm^{-3}], a =3.6·10^{-5} [s^{-1}], b =0.2γ [(eV cm^{-3})$^{-1/2}$], c =20γ, d = –1.5·10^{-3}γ [(mV m^{-1})$^{-1}$ s^{-1}].

The results of calculations of *Dst* and *AL* are shown in Figure 1, *b*. Under quiet conditions (B_z=0), *Dst*~0 nT, *AL*≈–34 nT. During the disturbed period (B_z=–7 nT), *Dst* and *AL* amount approximately to –50 and –500 nT respectively.

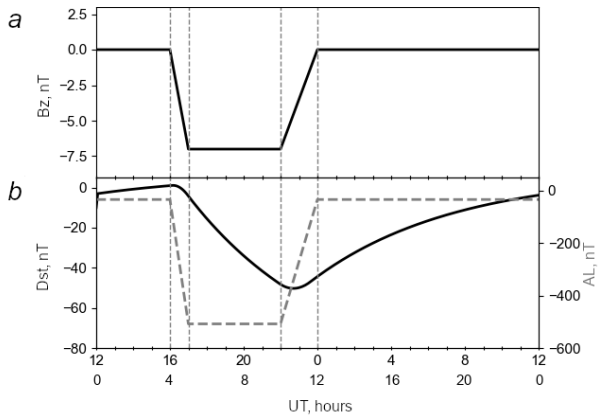

Figure 1. Variations in the IMF B_z component (*a*) and calculated geomagnetic activity indices *Dst* (solid line) and *AL* (dashed line) (*b*) at the storm sudden commencement at 16:00 UT and 04:00 UT

3. RESULTS AND DISCUSSION

Figure 2 illustrates space-time distributions of electron density at the height of the F2 maximum n_mF2 at different moments of UT under quiet (*a–f*) and disturbed (*g–l*) conditions. To make the convection effect more visible, we ignored charged particle precipitation. Concentric circles indicate geographic latitudes of the Northern Hemisphere drawn through 10°. The lower boundary corresponds to 40° N. The numbers on the outer circle are the local time, and the geographic longitude is shown in parentheses next to it. Referring to the figure, the Western Hemisphere is located on the dayside. The dashed line (top) is the position of the terminator at a zenith angle χ=90°. The point of intersection of two mutually perpendicular lines is the geomagnetic pole, which is 11.5° away from the geographic pole. Arrows in this figure, as well as in Figures 3–9, indicate velocity vectors of ionospheric plasma drift caused by the magnetospheric convection electric field (the longer the arrow, the higher the velocity). White isolines denote electric field potentials calculated using the Weimer model. Let us analyze the results of numerical calculations for quiet conditions (B_z=0) (see Figure 2, *a–f*). In this case, the convection structure consists of two cells in the dawn and dusk sectors (see Figure 2, *a*). The configurations of the isolines of the electric field potential and electron and ion drift velocities (arrows) show that at 16:00 UT the convection region partially enters the dayside zone above the terminator, which leads to antisunward plasma transfer from the dayside ionosphere to the nightside and to the formation of the tongue of ionization. Then, from 16:00 to 00:00 UT there is a gradual shift of the tongue of ionization toward the nightside due to Earth's rotation around its axis and the displacement between geographic and geomagnetic poles.

Figure 2, *g–l* presents the results of numerical calculations for disturbed conditions. The IMF B_z component is set according to scenario 1 (see Figure 1). At the initial moment of 16:00 UT, the convection electric field is seen to correspond to quiet conditions (B_z =0) (see Figure 2, *g*). Then, from 16:00 to 17:00 UT, due to a decrease in IMF B_z to –7 nT, convection is enhanced and the area of its action enlarges, which is clearly seen from isolines of the electric field potential (see Figure 2, *h*, *i*). This causes the area of overlap of the convection region with the dayside ionosphere to increase at 17:00 UT (see Figure 2, *i*) and hence to more significant plasma transfer from the dayside ionization to the nightside by the antisunward flow and the subsequent elongation of the tongue of ionization in the day–night direction at 19:00 UT (see Figure 2, *j*). Enhanced convection leads to an increase in n_mF2 in the nightside high-latitude ionosphere to values lager than 3·10^6 cm^{-3} (see Figure 2, *j*, *k*). In the dusk and dawn sectors in the regions of sunward convection, the plasma transfer is observed by noon (see Figure 2, *j*, *k*). After 22 UT, convection weakens, but on the nightside at 00:00 UT in high latitudes n_mF2 is higher than under quiet conditions due to residual ionization accumulated during the storm

main phase (see Figure 2, *f* and *l*). Thus, comparison between the results of numerical calculations for quiet and disturbed conditions shows that positive disturbances occur at subauroral and high latitudes during a moderate geomagnetic storm due to enhanced antisunward convection and increased area of its action.

Figure 3 presents the results of numerical calculations with regard to charged particle precipitation by APM PGIA [Vorobjev et al., 2013]. The calculated rates of corpuscular ionization are shown in Figure 4. In this case, the high-latitude ionosphere is additionally supported by ionization by incoming charged particles in the auroral oval. Under quiet conditions at 16:00 UT, a region of low n_mF2 is formed in the polar region ($\Phi_m \geq 80°$) — a polar hole (see Figure 3, *a*) surrounded by ionization in the auroral oval. In the latitude dependence in the dusk sector in the "full shadow" region

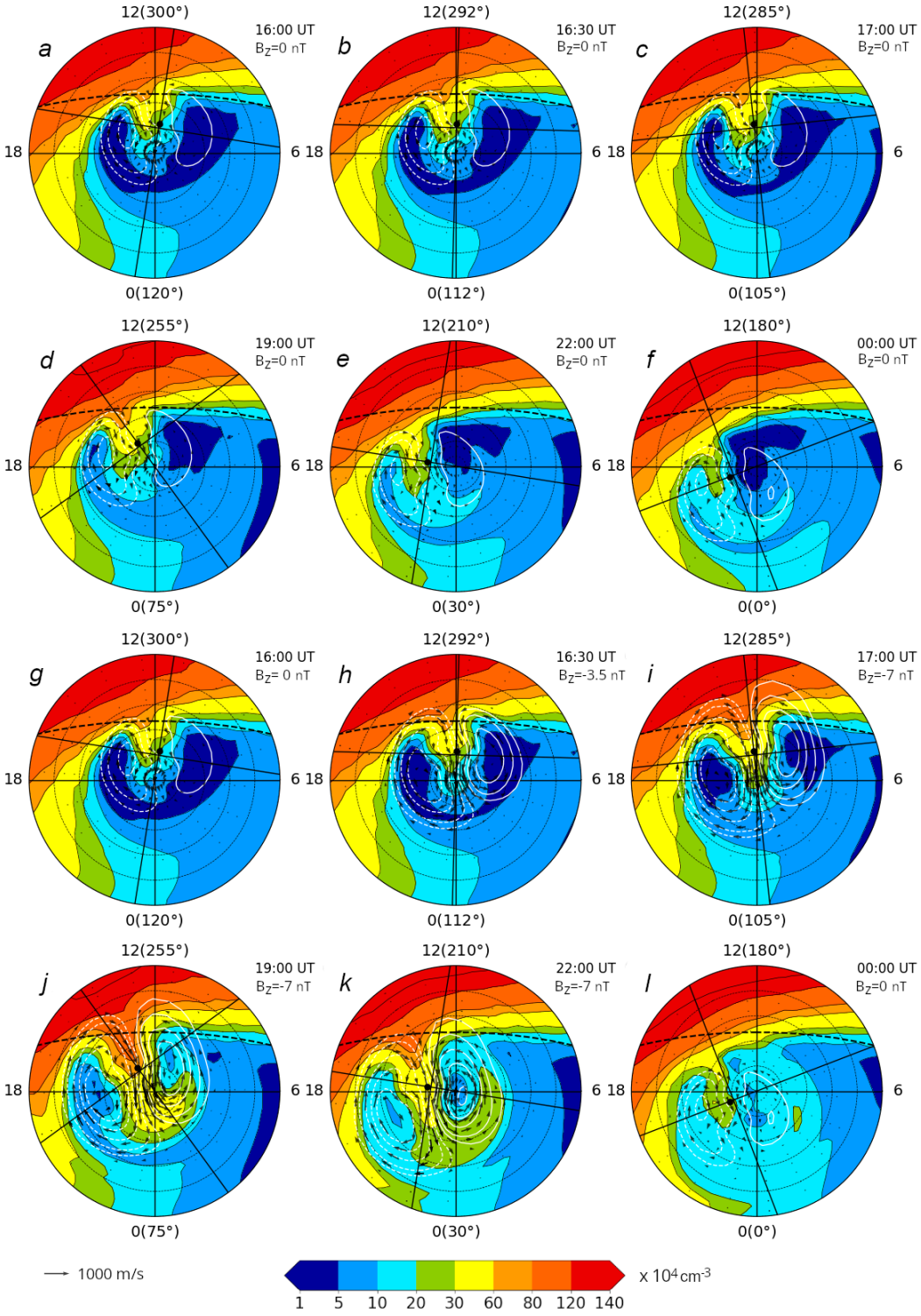

Figure 2. Space-time distributions of electron density at the height of the F2 maximum n_mF2 at different moments of UT under quiet (B_z=0, *a*–*f*) and disturbed ($B_z \neq 0$, *g*–*l*) conditions without regard to charged particle precipitation for a storm starting at 16:00 UT

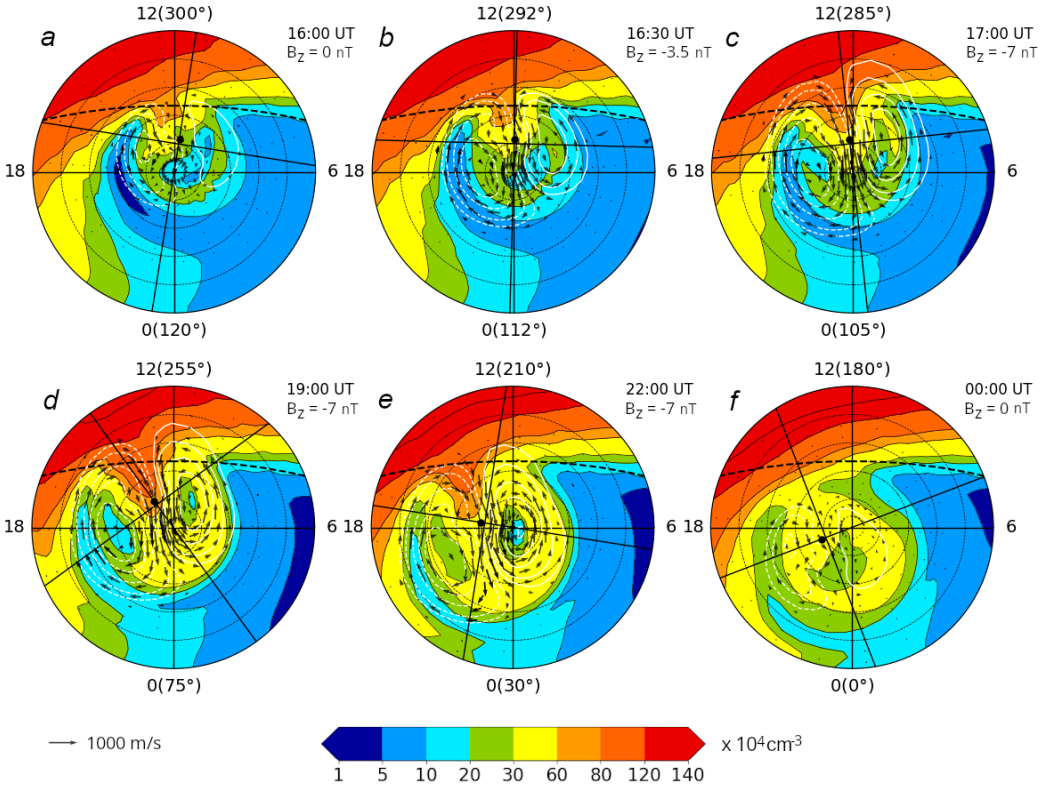

Figure 3. The same as in Figure 2, but with regard to charged particle precipitation

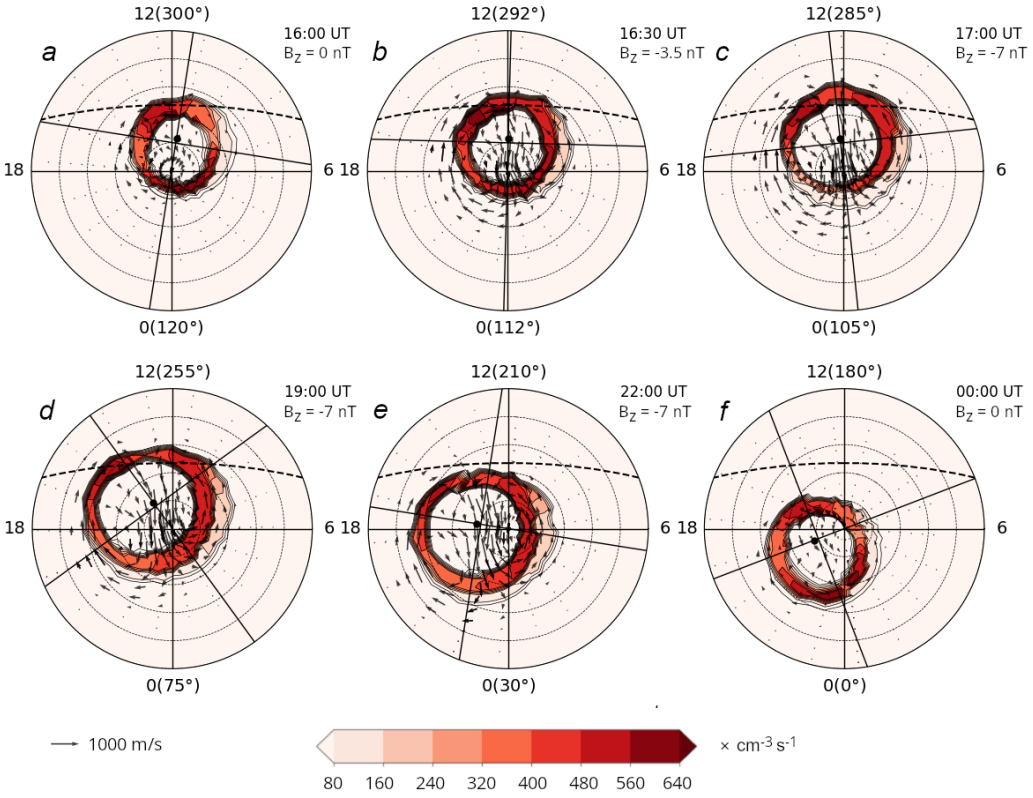

Figure 4. Space-time distributions of the rate of corpuscular ionization q_k calculated by APM PGIA [Vorobjev et al., 2013] at a height of 200 km (auroral oval)

[Kolesnik, Golikov, 1982], there is a deep trough of concentration — the main ionospheric trough (Figure 3, *a*). The polar wall of MIT is formed due to the combined action of corpuscular ionization and magnetospheric convection. After the onset of the storm at 16:30 UT, the perturbed convection electric field leads to disap-

pearance of the polar hole due to an expansion of ionized particle fluxes from the dayside into this region (see Figure 3, *b, c*). At 19:00 UT, the depth of MIT decreases, and its position shifts southward by ~5°÷10° (see Figure 3, *e*). The electron density n_e in the tongue of ionization increases. By 00:00 UT, IMF B_z drops to 0 nT, and the area of the convection region decreases and becomes the same as under quiet conditions (see Figure 3, *f*). Meanwhile, residual dayside ionization persists behind the convection and precipitation regions.

Let us now examine the response of the large-scale structure of the high-latitude ionosphere to a magnetic storm starting at 04:00 UT. This situation is diametrically opposite to that arisen during the magnetic storm starting at 16:00 UT. Figure 5 shows the results of numerical calculations for quiet and disturbed conditions in terms of charged particle precipitation. In this case,

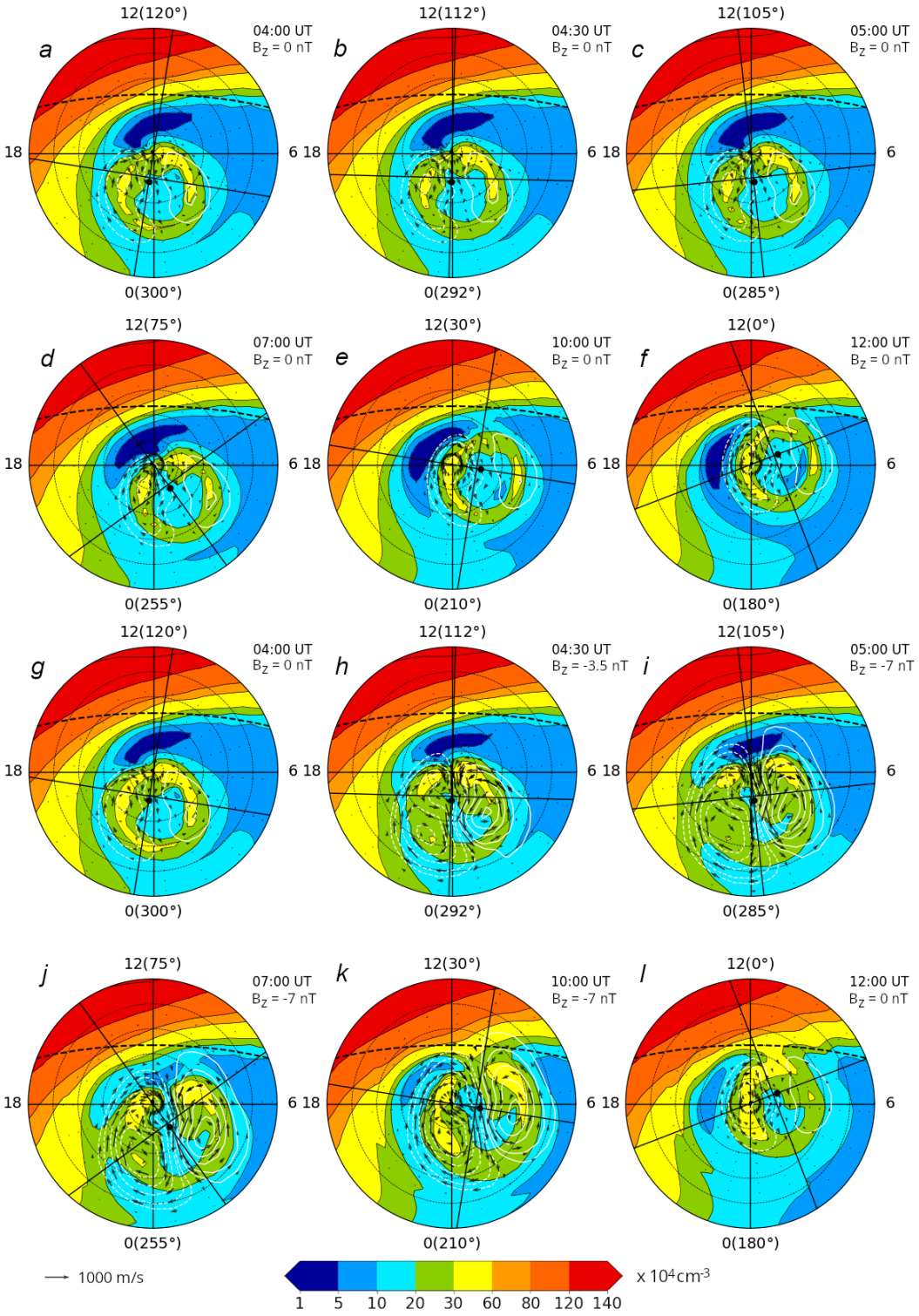

Figure 5. Space-time distributions of electron density at the height of the F2 maximum n_mF2 at different moments of UT under quiet (B_z=0, *a–f*) and disturbed ($B_z \neq 0$, *g–l*) conditions in terms of charged particle precipitation for the magnetic storm starting at 04:00 UT

the Eastern Hemisphere is on the dayside. As can be seen, at 04:00 UT the geomagnetic pole along with convection and precipitation regions is on the nightside. As a result, the tongue of ionization, the concentration in which is maintained by corpuscular ionization and magnetospheric convection, is separated from the dayside ionosphere (Figure 5, *a*). At geomagnetic latitudes above 80°, a polar hole with $n_m F2 \leq 10^4$ cm^{-3} is formed. In the latitude dependence on the dayside in the range 70–80° N, there is a deep trough of $n_m F2$ — the daytime trough (see Figure 5, *a–f*). The formation of the daytime trough in winter is associated with the "full shadow" phenomenon [Kolesnik, Golikov, 1984].

Under disturbed conditions, enhanced magnetospheric convection causes the separated tongue of ionization to expand and auroral peaks of $n_m F2$ to flatten (see Figure 5, *g–l*). At 07:00 UT, convection overlaps the daytime trough and significantly increases $n_m F2$ as compared to its values under quiet conditions (see Figure 5, *j*, *d*). By 12:00 UT, convection velocities fall and its region decreases. Nonetheless, comparison of Figure 5, *f* and *l* shows that residual dayside ionization persists on the nightside.

Thus, during a moderate magnetic storm, the magnetospheric convection effect, which leads to changes in shapes and sizes of the main large-scale structural features of the ionosphere, is determined by the time of onset of the geomagnetic storm due to the displacement between geographic and geomagnetic poles.

The effect of the storm is most pronounced if it starts at 16:00 UT. In this case, the perturbed electric field of magnetospheric convection transfers plasma from the dayside ionosphere to the nightside more intensively than under quiet conditions. A similar effect should occur in the Southern Hemisphere, where the displacement between geographic and geomagnetic poles is even greater. Note that the conditions of the nightside winter ionosphere in the region of closed field lines are affected by the ion flux from the conjugate summer ionosphere of the Southern Hemisphere. However, the diffusion transfer between conjugate ionospheres through the plasmasphere is characterized by inertia and is formed within ~8–10 hrs [Krinberg, Tashchilin, 1984].

As shown above, magnetospheric convection is one of the main mechanisms of horizontal plasma transfer at high and subauroral latitudes. Owing to the configuration of geomagnetic field lines, the convection electric field can also lead to upward and downward plasma drift together with plasma motion along the field lines due to diffusion and neutral wind [Klimenko, Namgaladze, 1976; Mingalev, 1978; Deng, Ridley, 2006; Schunk, Nagy, 2009; Liu et al., 2017]. Figure 6 illustrates space-time distributions of the vertical **E**×**B**-drift velocity.

$$u_{rE} = \frac{E_\phi}{H} \cos I,$$

where H is the magnetic field strength; I is the geomagnetic field inclination; E_φ is the zonal convection electric field component [Kolesnik, Golikov, 1982], calculated for conditions with the onset of the storm at 16:00 UT. At 16:00 UT under quiet conditions, u_{rE} is directed upward on the dayside (~+20 m/s) and downward on the nightside (~–20 m/s). At 19:00 UT under disturbed conditions, u_{rE} increases significantly and reaches about ±80 m/s. When comparing the u_{rE} distributions for 16:00 and 00:00 UT, we can see that u_{rE} depends on UT due to the displacement between geographic and geomagnetic poles. So, at the distribution for 16:00 UT on the nightside, u_{rE} is directed downward from 08:00 to 14:00 LT; whereas at the distribution for 00:00 UT, from 20:00 to 01:00 LT.

Figures 7, 8 demonstrate space-time distributions of $n_m F2$ and the height of the F2-layer maximum $h_m F2$ with and without regard to u_{rE}, calculated for the storm starting at 16:00 UT. Comparison of Figure 7, *a–c* with *d–f* allows us to estimate the effect of vertical electromagnetic drift. We can see that at 16:00 UT under quiet conditions the results of numerical calculations differ slightly (Figure 7, *a*, *d*). Yet, at 19:00 UT, after the start of the storm, the impact of u_{rE} causes $h_m F2$ to change significantly (Figure 8, *e*). On the dayside in the afternoon sector, the F2 layer rises to ~360 km; and on the nightside, it descends to ~220 km (see Figure 8, *e*). On the nightside, the effect of u_{rE} leads to a general decrease in $n_m F2$ in the subauroral and high-latitude ionosphere (see Figure 7, *e*, *f*). On the dayside, there is an increase in $n_m F2$ in the afternoon sector (Figure 7, *e*).

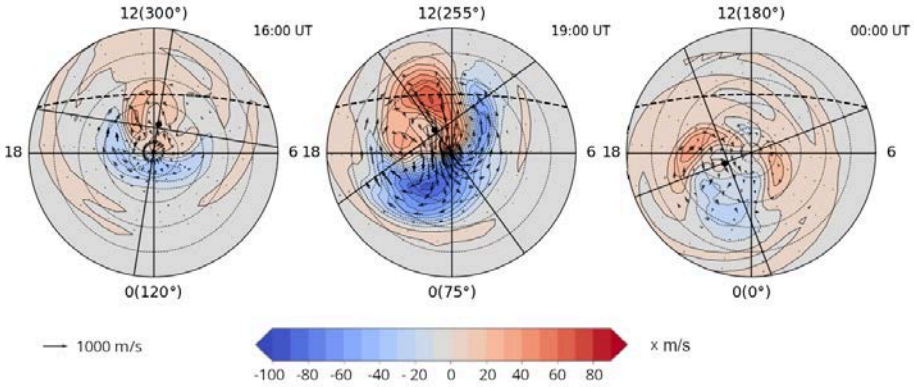

Figure 6. Space-time distributions of the vertical **E**×**B**-drift velocity component u_{rE} at a height of 300 km at different moments of UT

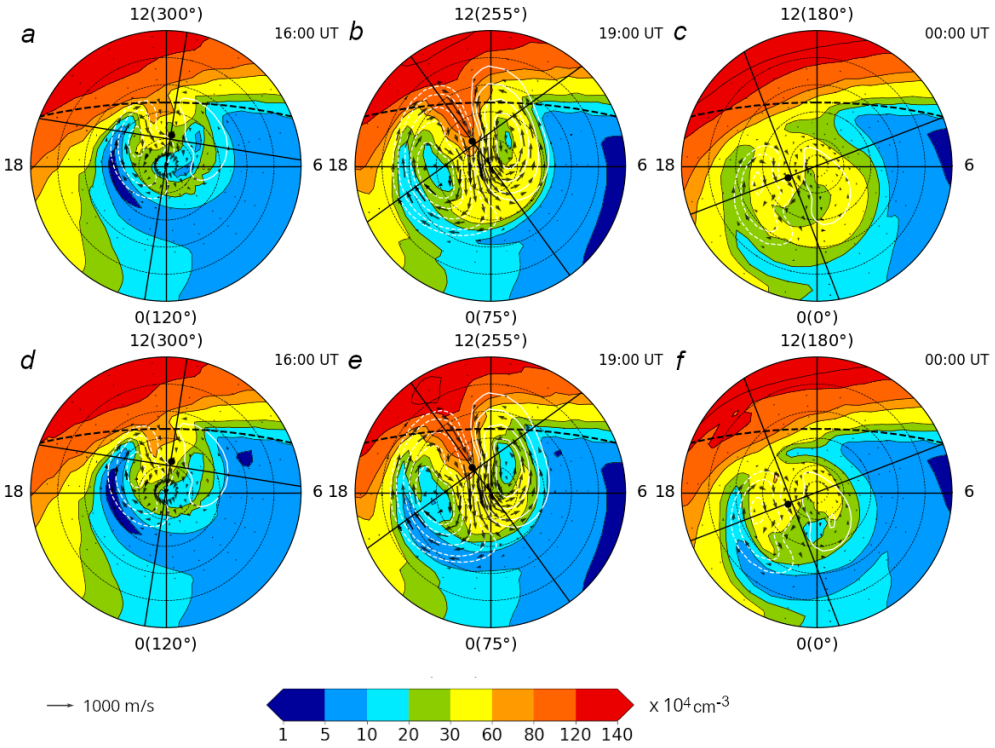

Figure 7. Space-time distributions of the maximum electron density in the F2 layer n_mF2 without (*a–c*) and with (*d–f*) regard to the vertical **E**×**B**-drift component u_{rE} at different moments of UT

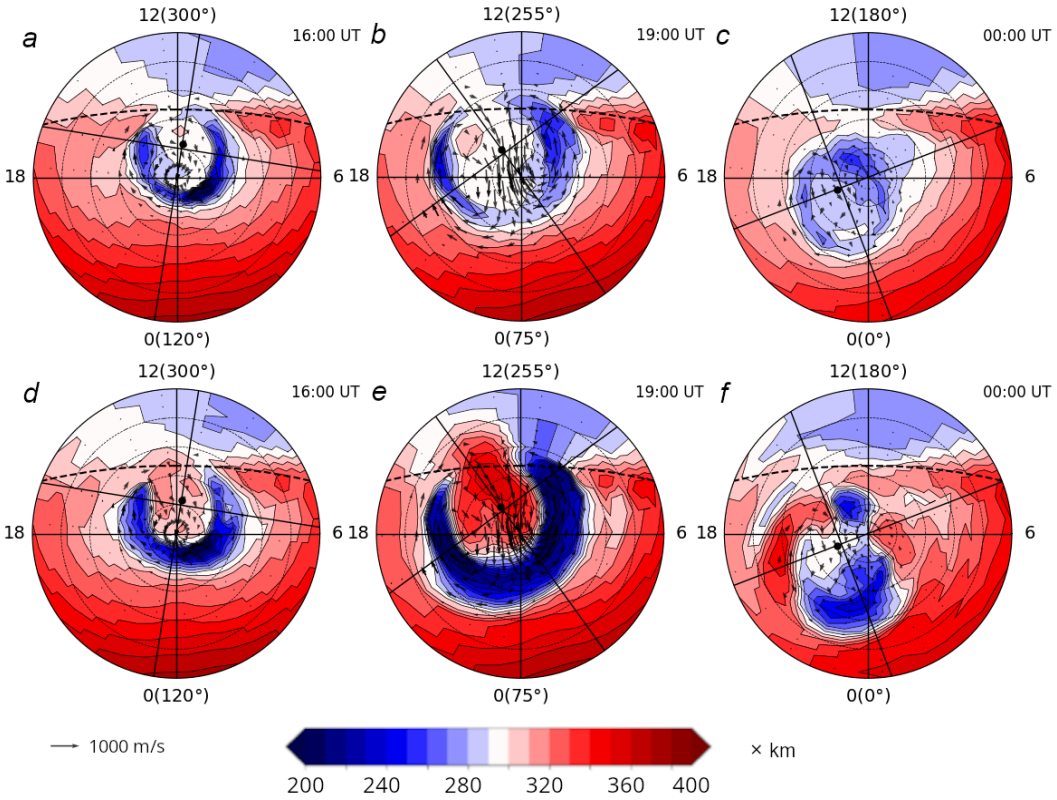

Figure 8. Space-time distributions of h_mF2 without (*a–c*) and with (*d–f*) regard to the vertical **E**×**B**-drift component u_{rE} at different moments of UT

At 00:00 UT, a polar hole with n_mF2≈10^5 cm^{-3} is formed at geomagnetic latitudes above ~80°, and h_mF2 decreases by 40 km compared to quiet conditions (from 300 to 260 km) (see Figures 7, *f*, 8, *f*). This indicates a connection between the formation of the polar hole and downward u_{rE}, which is consistent with the assumption put forward in [Tashchilin, Romanova, 2002].

Figures 9 and 10 illustrate the space-time distribution of electron density at 360 km and the vertical profile of n_e at 19:00 UT for day and night conditions with and without regard to u_{rE}. We can see that when u_{rE} is taken into account on the dayside in the afternoon sector above the terminator there is an increase in n_e due to the rise of the F2-layer maximum to the region where the recombination rate is lower (see Figures 9, *b*, 10, *a*). The density increase is hindered by the diffusion increase D_a at high altitudes, where plasma rises at a rate of u_{rE} (see Figure 10, *a*). On the nightside, there is a drop in n_e due to the descent of the layer to the region with a high density of neutral particles and hence with a higher recombination rate (see Figures 9, *b*, 10, *b*). Similar changes in h_mF2 and n_e in the region of perturbed magnetospheric convection were also observed from measurements with the incoherent scatter radar in Poker Flat and from global maps of the total electron content (TEC) of GPS during the October 24–25, 2011 geomagnetic storm [Zou et al., 2013].

Thus, the vertical component of the **E**×**B**-drift velocity has a significant effect on the large-scale structure of the ionosphere; therefore, its consideration is necessary when modeling the subauroral and high-latitude ionosphere during geomagnetic disturbances. Note that the effect caused by u_{rE} will depend on season, universal time, and type of convection. This issue requires further research.

CONCLUSION

We have studied the effect of magnetospheric convection on the large-scale structure of the ionosphere during a moderate geomagnetic storm for winter conditions (δ=–23°) through numerical calculations by the non-stationary ionosphere model in Eulerian variables.

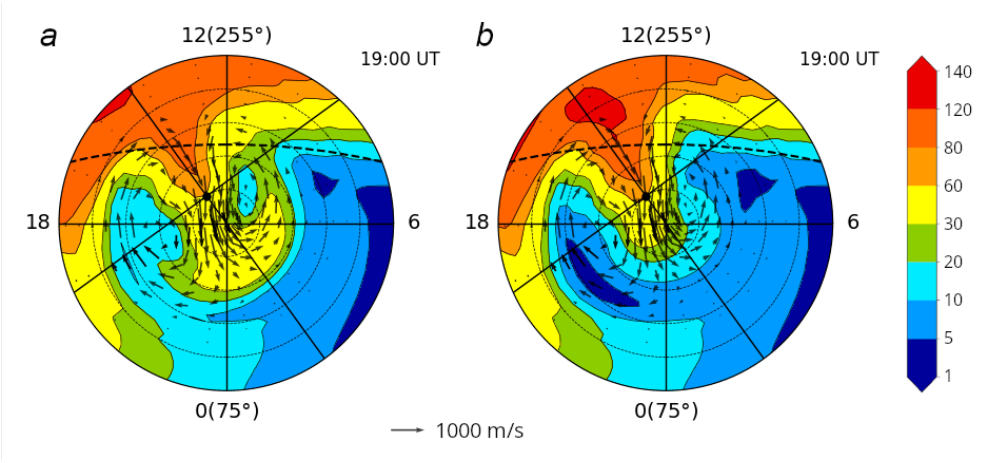

Figure 9. Space-time distributions of electron density n_e (10 cm^{-3}) at 360 km without (*a*) and with (*b*) regard to u_{rE}

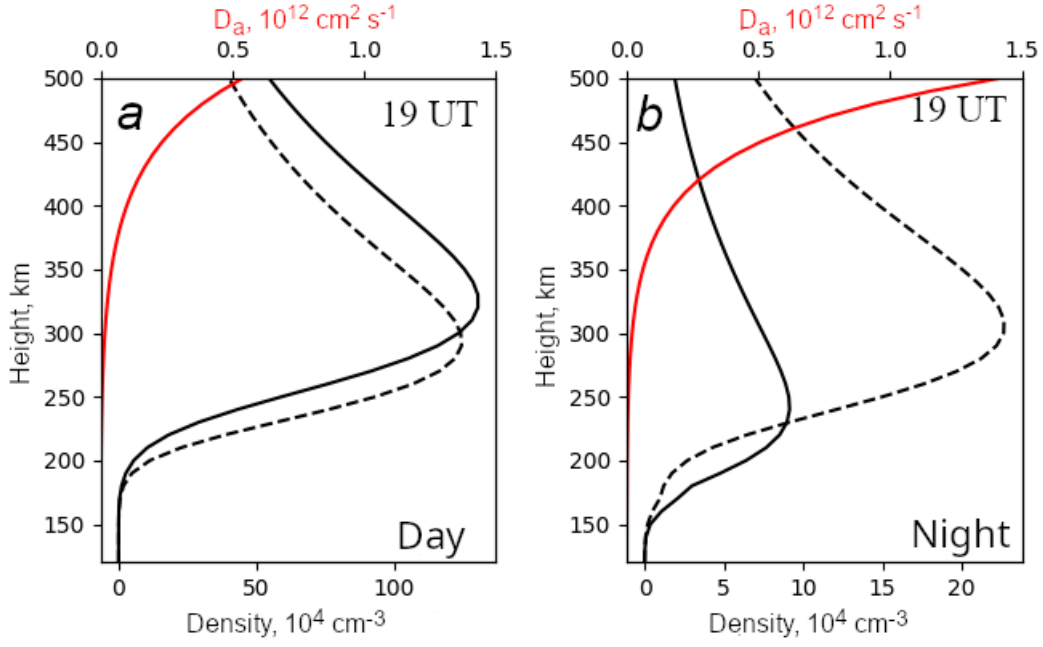

Figure 10. Vertical profiles of electron density n_e (black line) and ambipolar diffusion coefficient D_a (red line) at 19:00 UT for daytime (54° N, 280° E) and nighttime conditions (70° N, 60° E) without (dashed line) and with (solid line) regard to u_{rE}

The results of the study allow us to draw the following conclusions:

1. Disturbance of the magnetospheric convection electric field during a moderate geomagnetic storm causes changes in shapes and sizes of the main structural features of the ionosphere such as the polar hole, the tongue of ionization, and the main ionospheric trough.

2. In winter, the geomagnetic storm effect depends on the time of onset of the disturbance (UT control) due to the displacement between geographic and geomagnetic poles. The effect is most pronounced in the case of a storm starting at 16:00 UT when the perturbed magnetospheric convection electric field transfers plasma from the dayside ionosphere to the nightside.

3. During disturbed periods, the vertical electromagnetic drift component has a significant effect on the large-scale structure of the ionosphere, which causes the electron density to decrease on the nightside and to increase on the dayside due to a change in the height of the layer maximum.

The work was carried out under government assignment (State Registration Number 122011700182-1).

REFERENCES

Burton R.K., McPherron R.L., Russel C.T. An empirical relationship between interplanetary conditions and *Dst*. *J. Geophys. Res*. 1975, vol. 80, no. 31. pp. 4204–4214. DOI: 10.1029/JA080i031p04204.

Chapman S. The absorption and dissociative of ionizing effect of monochromatic radiation in an atmosphere on a rotation. *Earth. Proc. Phys. Soc*. 1931, vol. 43. pp. 483–501. DOI: 10.1088/0959-5309/43/5/302.

Danilov A.D. Reaction of F region to geomagnetic disturbances (review). *Geliogeofizicheskie issledovaniya* [Helio-Geophysic Research]. 2013, no. 5, pp. 1–33. (In Russian).

David M., Schunk R. Sojka J. The effect of downward electron heat flow and electron cooling processes in the high-latitude ionosphere. *J. Atmos. Solar-Terr. Phys*. 2011, vol. 73, pp. 2399–2409. DOI: 10.1016/j.jastp.2011.08.009.

Deng Y., Ridley A.J. Role of vertical ion convection in the high-latitude ionospheric plasma distribution. *J. Geophys. Res*. 2006, vol. 111, A09314. DOI: 10.1029/2006JA011637.

Evans J.V. *Millstone Hill Thomson scatter results for 1969*. *Technical Report 513*. Massachusetts Institute of Technology, 1974, 140 p.

Fang X., Randall C., Lummerzheim D., Solomon S., Mills M.J., Marsh D.R., et al. Electron impact ionization: A new parameterization for 100 eV to 1 MeV electrons. *J. Geophys. Res*. 2008, vol. 113, iss. 9. DOI: 10.1029/2008JA013384.

Golikov I.A., Gololobov A.Yu., Popov V.I. Numerical simulation of thermal regime of high-latitude ionosphere. *Vestnik Severo-Vostochnogo federal'nogo universiteta* [Vestnik of North-Eastern Federal University]. 2012, vol. 9, no. 3, pp. 22–28. (In Russian).

Golikov I.A., Gololobov A.Yu., Popov V.I. Modelling the electron temperature distribution in F2 region of high-latitude ionosphere for winter solstice. *Solar-Terr. Phys*. 2016, vol. 2, iss. 4, pp. 54–62. DOI: 10.12737/24269.

Golikov I., Gololobov A., Baishev D. Universal time control of the parameters of the electron temperature enhancement zone in the winter subauroral ionosphere. *J. Atmos. Solar-Terr. Phys*. 2020, vol. 211. DOI: 10.1016/j.jastp.2020.105458.

Golikov I., Gololobov A., Baishev D., Makarov G. Determination of the enhancement in electron temperature in the subauroral ionosphere during magnetic storms on a global scale. *Geomagnetism and Aeronomy*. 2022, vol. 61, suppl. 1, pp. S103–S115. DOI: 10.1134/S001679322201008X.

Heppner J.P., Maynard N.C. Empirical high-latitude electric field models. *J. Geophys. Res*. 1987, vol. 92, pp. 4467–4489.

Klimenko V.V., Namgaladze A.A. The effects of zonal electric field in the daytime winter midlatitude ionosphere. *Geomagnetizm i ajeronomija* [Geomagnetism and aeronomy]. 1976, vol. 16, pp. 1117–1119. (In Russian).

Klimenko M.V., Klimenko V.V., Bessarab F.S., Ratovsky K.G., Zakharenkova I.E., Nosikov I.A., Stepanov A.E., et al. Influence of geomagnetic storms of September 26–30, 2011, on the ionosphere and HF radiowave propagation. I. Ionospheric effects.*Geomagnetism and Aeronomy*. 2015, vol. 55, no. 6, pp. 744–762.

Klimenko M.V., Zakharenkova I.E., Klimenko V.V., Lukianova R.Yu., Cherniak I.V. Simulation and observation of the polar tongue of ionization at different heights during the 2015 St. Patric's day storms. *Space Weather*. 2019, vol. 17, pp. 1073–1089. DOI: 10.1029/2018SW002143.

Kolesnik A.G., Golikov I.A. Study of the role of various mechanisms in formation of the F2 region of the ionosphere on a two-dimensional model *Geomagnetizm i ajeronomiya* [Geomagnetism and Aeronomy]. 1981, vol. 21, no. 4, pp. 612–616. (In Russian).

Kolesnik A.G., Golikov I.A. Three-dimensional model of the high-latitude F region with taking into account the mistmach of geographic and geomagnetic coordinates. *Geomagnetizm i ajeronomiya* [Geomagnetism and Aeronomy], 1982, vol. 22, no 3, pp. 435–439. (In Russian).

Kolesnik A.G., Golikov I.A. The "full shadow" phenomena in Earth upper atmosphere. *Doklady AN SSSR* [Report of Academy of Sciences USSR]. 1984, vol. 279, no. 4, pp. 832–834. (In Russian).

Krinberg I.A., Taschilin A.V.*Ionosfera i plazmosfera* [Ionosphere and Plasmasphere]. Moscow, Nauka Publ., 1984, p. 190. (In Russian).

Larina T.N., Glebova G.M. Investigation of electron density variation in the polar ionosphere F-layer influenced by interplanetary magnetic field B_y component sign. *Inzhenernyi vestnik Dona* [Engineering Bull. of Don]. 2019, vol. 1, 11 p. URL: http://www.ivdon.ru/uploads/article/pdf/IVD_120__larina_N.pdf_5a3560990a.pdf (accessed January 10, 2025).

Liu J., Wang W., Burns A., Liu L., McInerney J. A TIEGCM numerical study of the source and evolution of ionospheric F-region tongues of ionization: Universal time and interplanetary magnetic field dependence. *J. Atmos. Solar-Terr. Phys*. 2017, vol. 156, pp. 87–96. DOI: 10.1016/j.jastp.2017. 03.005.

Lukianova R.Yu., Uvarov V.M., Coisson P. High-latitude F region large-scale ionospheric irregularities under different solar wind and zenith angle conditions. *Adv. Space. Res*. 2016, vol. 59, pp. 557–570. DOI: 10.1016/j.asr.2016.10.010.

Mingalev V.S. Electric field influence on the polar ionosphere. *Polyarnaya ionosfera i magnitosferno-ionosfernye svyazi* [Polar ionosphere and magnetosphere-ionosphere coupling]. Apatity, 1978, pp. 43–48. (In Russian).

Mizun Yu.G. *Polyarnaya ionosfera* [Polar ionosphere]. Leningrad, Nauka Publ., 1980, 216 p. (In Russian).

Murayama T. Coupling function between solar wind parameters and geomagnetic indices. *Rev. Geophys. Space Phys*. 1982, vol. 20, no. 3, pp. 623–629. DOI: 10.1029/RG020i003p00623.

Murayama T., Aoki T., Nakai H., Hakamada K. Empirical formula to relate the auroral electrojet intensity with interplane-

tary parameters. *Planet Space. Sci.* 1980, vol. 28, pp. 803–813.DOI: 10.1016/0032-0633(80)90078-1.

Picone J.M., Hedin A.E., Drob D.P. Aikin A. NRLMSISE-00 empirical model of the atmosphere: Statistical comparison and scientific issues. *J. Geophys. Res.* 2002, vol. 107, pp. 1501–1516. DOI: 10.1029/2002JA009430.

Prölss G.W. *Ionospheric F-region storms. Handbook of Atmospheric Electrodynamics II*. Eds. H. Volland. Boca Raton, CRC Press, 1995, pp. 195–248.

Ratovsky K.G., Klimenko M.V., Klimenko V.V., Chirik N.V., Korenkova N.A., Kotova D.S. After-effects of geomagnetic storms: statistical analysis and theoretical explanation. *Solar-Terr. Phys.* 2018, vol. 4, iss. 4, pp. 26–32. DOI: 10.12737/stp-44201804.

Samarskii A. *The Theory of Difference Schemes*. New York, Marcel Dekker, 2001, 761 p.

Schunk R., Nagy A. Electron temperature in the F regions of the ionosphere: theory and observations. *Rev. Geophys.* 1978, vol. 16, pp. 355–399. DOI: 10.1029/RG016i003p00355.

Schunk R.W., Nagy A. *Ionospheres: Physics, Plasma Physics, and Chemistry*. New York, Cambridge University Press, 2009, 628 p.

Sojka J.J., Raitt W.J., Schunk R.W. Effect of displaced geomagnetic and geographic poles on high-latitude plasma convection and ionospheric depletions. *J. Geophys. Res*. 1979, vol. 85, no. A10, pp. 5943–5951. DOI: 10.1029/JA084iA10p05943.

Tashchilin A.V., Romanova E.B. Numerical modeling the high-latitude ionosphere. *Proc. of the COSPAR Colloquim on Solar-Terrestrial Magnetic Activity and Space Environment (STMASE). Beijing, China.* Pergamon, 2002, vol. 14, pp. 315–325.

Tashchilin A.V., Romanova E.B. Influence of magnetospheric inputs definition on modeling of ionospheric storms. *Physics of Auroral Phenomena, Proc. XXX Annual Seminar*, 2007, pp. 189–192.

Uvarov V.M., Barashkov P.D. The electric field distribution types and related convection types in the polar ionosphere. Model.*Geomagnetizm i ajeronomiya* [Geomagnetism and Aeronomy]. 1989, vol. 29, no. 4, pp. 621–628. (In Russian).

Uvarov V.M., Lukianova R.Yu. The high-latitude ionosphere modelling with considering interplanetary medium.*Geliogeofizicheskie issledovaniya* [Helio-geophysical research]. 2014, no 7, pp. 108–118. (In Russian).

Uvarov V.M., Lukianova R.Yu. Numerical modeling of the polar F region ionosphere taking into account the solar wind conditions. *Adv. Space. Res.* 2015, vol. 56, no. 11, pp. 2563–2574. DOI: 10.1016/j.asr.2015.10.004.

Vorobjev V.G., Yagodkina O.I., Katkalov Yu.V. Auroral Precipitation Model and its application to ionospheric and magnetospheric studies. *J. Atmos. Solar-Terr. Phys.* 2013, vol. 102, pp. 157–171. DOI: 10.1016/j.jastp.2013.05.007.

Watkins B.J. A numerical computer investigation of the polar F-region ionosphere. *Planet. Space Sci*. 1978, vol. 26, pp. 559–569. DOI: 10.1016/0032-0633(78)90048-X.

Weimer D.R. A flexible, IMG dependent model of high-latitude electric potentials having “space weather” applications. *Geophys. Res. Lett.* 1996, vol. 23, no. 18. pp. 2549–2552.

Yermolaev Yu.I., Lodkina I.G., Nikolaeva N.S., Yermolaev M.Yu. Statistical study of interplanetary condition effect on geomagnetic storms: 2. Variations of parameters. *Cosmic Res.* 2011, vol. 49, no 1, pp. 21–34. DOI: 10.1134/S0010 952511010035.

Zherebtsov G.A., Mizun Yu.G., Mingalev V.S. *Fizicheskie protsessy v polyarnoi ionosfere* [Physical processes in the polar ionosphere]. Moscow, Nauka Publ., 1988, 231 p. (In Russian).

Zou S., Ridley A., Moldwin M.B., Nicolls M.J., Coster A.J., Thomas E.G., Ruohoniemi J.M. Multi-instrument observations of SED during 24-25 October 2011 storm: Implications for SED formation processes. *J. Geophys. Res.: Space Phys.* vol. 118. pp. 7798–7809. DOI: 10.1002/2013JA018860.

URL: http://omniweb.gsfc.nasa.gov (accessed January 10, 2025).

Original Russian version: Gololobov A.Yu., Golikov I.A., Popov V.I., published in Solnechno-zemnaya fizika. 2025, vol. 11, no. 2, pp. 100–111. DOI: 10.12737/szf-112202509.

How to cite this article

Gololobov A.Yu., Golikov I.A., Popov V.I. Modelling the influence of magnetospheric storm on the large-scale structure of the high-latitude ionosphere for winter solstice conditions. *Sol.-Terr. Phys*. 2025, vol. 11, iss. 1, pp. 88–98. DOI: 10.12737/stp-112202509.